JET PRODUCTION IN PHOTON-PHOTON INTERACTIONS *

STEFAN SÖLDNER-REMBOLD

Albert-Ludwigs-Universität Freiburg, Fakultät für Physik, D-79104 Freiburg im Breisgau, Germany

On behalf of the OPAL collaboration

The inclusive one- and two-jet cross-sections are measured in collisions of quasi-real photons at e^+e^- centre-of-mass energies $\sqrt{s}_{ee}$ = 130 and 136 GeV using the OPAL detector at LEP. Jets are reconstructed with a cone jet finding algorithm. The jet cross-sections are compared to next-to-leading order (NLO) perturbative QCD calculations. Transverse energy flows in jets are studied separately for direct and resolved two-photon events.

1 Introduction

We present measurements of jet production in $\gamma\gamma$ interactions at $\sqrt{s}_{ee}$ of 130 and 136 GeV. The jet cross-sections are compared to predictions of perturbative QCD which use different parametrisations of the photon structure function.

In the Quark Parton Model (QPM) jets are produced by the interaction of bare photons, $\gamma\gamma \to q\overline{q}$. This is called the direct process. The largest part of the total cross-section, however, is modelled by interactions where the photon fluctuates into a hadronic state. The processes are called single-resolved if one photon couples directly to a parton in the other photon and double-resolved if partons from both photons interact.

2 Data analysis and Monte Carlo simulation

Two-photon events are selected by requiring that the sum of all energy deposits in the calorimeters is less than 50 GeV. The hadronic invariant mass, W_{ECAL}, measured in the electromagnetic calorimeter has to be greater than 3 GeV; the missing transverse energy of the event has to be less than 5 GeV; at least 5 charged tracks must have been found and no track may have a momentum greater than 15 GeV/c.

To remove events with scattered electrons in the forward detectors, the energy measured in these detectors has to be less than 40 GeV (20 GeV) depending on the angular range, corresponding to an effective maximum photon virtuality, Q^2_{max}, of 0.8 GeV^2 ("anti-tagging condition").

For an integrated luminosity of 4.9 pb^{-1}, 7808 events remain after all cuts. The average visible hadronic invariant mass W_{vis} is about 18 GeV. The total background from other processes is about 1 %.

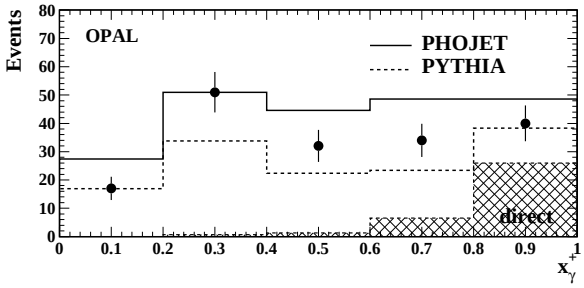

Figure 1: The number of two-jet events as a function of x_γ^+ compared to PHOJET and PYTHIA. Statistical errors only are shown. The hatched histogram is the direct contribution to the PYTHIA events.

The leading order (LO) QCD generators PYTHIA 5.721 [1] and PHOJET 1.05 [2] are used for the $\gamma\gamma$ event simulation. The fragmentation is handled by JETSET 7.408 [1].

3 Jet reconstruction and backgrounds

In the cone jet finding algorithm a jet is defined as a set of particles, i. e. partons or hadrons generated in a Monte Carlo program, or tracks and calorimeter clusters, whose momenta lie within a cone of size R, such that the axis of the cone coincides with the momentum sum of the particles contained. The cone size R, which is chosen to be $R = 1$, is defined as $R = \sqrt{(\Delta\eta)^2 + (\Delta\phi)^2}$, with $\eta = -\ln\tan(\theta/2)$ being the pseudorapidity and ϕ the azimuthal angle in the laboratory frame. $\Delta\eta$ and $\Delta\phi$ are the differences between the cone axis and the particle direction. The total transverse energy E_T^{jet} of the jet (defined with respect to the

*To be published in the proceedings of ICHEP'96, Warsaw

beam axis) is the scalar sum of the transverse energies E_{T_i} of its components. The pseudorapidity $\eta^{\rm jet}$ and the azimuthal angle $\phi^{\rm jet}$ are defined as the sum over the η_i and ϕ_i of the jet components weighted by their transverse energies E_{T_i}:

$$\eta^{\rm jet} = \frac{\sum_i E_{T_i}\eta_i}{\sum_i E_{T_i}} \quad \text{and} \quad \phi^{\rm jet} = \frac{\sum_i E_{T_i}\phi_i}{\sum_i E_{T_i}}.$$

All results are given for jets with $E_T^{\rm jet} > 3$ GeV and $|\eta^{\rm jet}| < 1$.

4 Energy flow in jet events

In γp scattering, direct and resolved two-jet events, which correspond to the single- and double-resolved events in $\gamma\gamma$ scattering if the proton is substituted in the place of a VMD-like photon, have been identified by measuring the fraction x_γ of the photon energy participating in the hard scattering[3]. In $\gamma\gamma$ scattering two photons interact, therefore a pair of variables is defined [4]

$$x_\gamma^\pm = \frac{\sum_{\rm jets}(E \pm p_z)}{\sum_{\rm hadrons}(E \pm p_z)}, \qquad (1)$$

where p_z is the momentum component along the z axis of the detector and E is the energy. Ideally, the total energy of the event is contained in the two jets for direct events without remnant jets, i. e. $x_\gamma^\pm = 1$, whereas for resolved events at least one of the $x_\gamma^\pm$ values is expected to be much smaller than one. The variables $x_\gamma^\pm$ are measured using all tracks and calorimeter clusters that were used in the jet finding algorithm. In addition, the energies in the forward detectors, which are not used for jet finding and for the energy flow distributions, are added in the denominator of Eq. 1. This improves the separation of direct and resolved events.

Figure 1 shows the number of two-jet events as a function of x_γ^+, together with the PYTHIA and PHOJET samples, after the detector simulation. The x_γ^- distribution, which is not shown, is consistent with the x_γ^+ distribution within the statistical errors. The peak expected for direct events at $x_\gamma^+ = 1$ is smeared out due to higher order QCD, hadronisation and detector resolution effects. Only statistical errors are shown, since systematic effects largely cancel in the ratio (Eq. 1).

The direct events, which are shown separately for the PYTHIA sample, mainly contribute

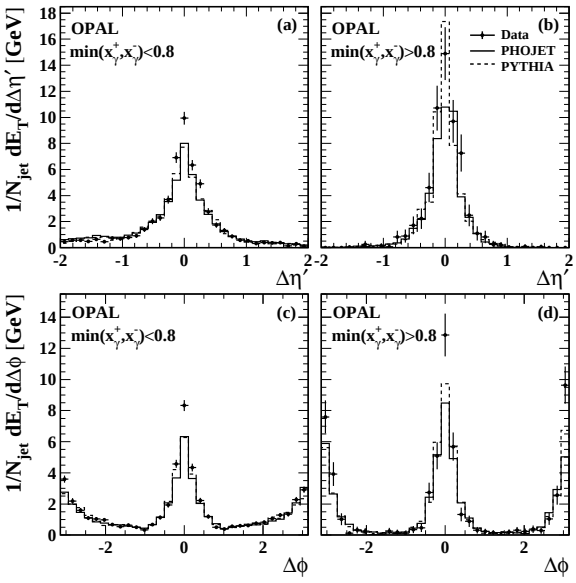

Figure 2: Transverse energy flow measured relative to the direction of the jet in two-jet events. Jets from events with $\min(x_\gamma^+, x_\gamma^-) < 0.8$ (a,c) and $\min(x_\gamma^+, x_\gamma^-) > 0.8$ (b,d) are shown separately. The energy flow is integrated over $|\Delta\phi| < \pi/2$ for the $\Delta\eta'$ projection (a,b) and over $|\Delta\eta'| < 1$ for the $\Delta\phi$ projection (c,d). Statistical errors only are shown.

in the region $x_\gamma^+ > 0.8$. Experimentally, samples with large and small direct contributions are separated by requiring $\min(x_\gamma^+, x_\gamma^-) > 0.8$ and $\min(x_\gamma^+, x_\gamma^-) < 0.8$, respectively. About 95 % of all events in the region $\min(x_\gamma^+, x_\gamma^-) > 0.8$ originate from direct interactions in PYTHIA.

Figure 2 shows the transverse energy flows

$$\frac{1}{N_{\rm jet}}\frac{{\rm dE_T}}{{\rm d}(\Delta\eta')} \quad \text{and} \quad \frac{1}{N_{\rm jet}}\frac{{\rm dE_T}}{{\rm d}(\Delta\phi)} \qquad (2)$$

with respect to the jet direction for two-jet events with $\min(x_\gamma^+, x_\gamma^-) < 0.8$ (low x_γ) and with $\min(x_\gamma^+, x_\gamma^-) > 0.8$ (high x_γ), separately. The shape of the selected jet is seen clearly in both $\Delta\eta'$ and $\Delta\phi$. No detector correction has been applied. The same tracks and clusters which are used for jet finding are included, with

$$\Delta\eta' = k(\eta - \eta^{\rm jet}) \ \text{ and } \ \Delta\phi = \phi - \phi^{\rm jet}. \qquad (3)$$

The rapidity difference is multiplied by a factor $k = \pm 1$. The factor k is chosen event-by-event to be $k = +1$ for events with $x_\gamma^+ > x_\gamma^-$ and $k = -1$ for events with $x_\gamma^+ < x_\gamma^-$. Due to the choice of k, there is always more energy flow at $\Delta\eta' < 0$.

In Fig. 2, a pedestal is observed which could indicate the existence of a photon remnant. As expected, this enhancement in the region around $|\Delta\phi| \approx \pi/2$ and at $|\Delta\eta'| > 1$ is more pronounced for low x_γ events. The jets in high x_γ events are much more back-to-back in $\Delta\phi$ (Fig. 2d) than in low x_γ events (Fig. 2c). The pedestal in the $\Delta\phi$ region between the two jets at $|\Delta\phi| \approx \pi/2$ is not observed in the high x_γ events. Jets in high x_γ events are also observed, on average, to have more average transverse energy and to be more collimated. This is as expected for direct events, where all the available energy is used in the hard subsystem. Both Monte Carlo models describe the transverse energy flow reasonably well, except for an underestimate in the central region around the jet axis. Nevertheless the overall modelling is sufficiently good to justify using the Monte Carlo models for unfolding the detector resolution effects in the jet cross-section measurements.

5 Inclusive jet cross-sections

The one- and two-jet cross-sections shown in Fig. 3 are corrected to the hadron level using the method of regularised unfolding. The main systematic uncertainty on the jet cross-sections originates from varying the energy scale of the ECAL in the Monte Carlo simulation by ± 5 % and from the unfolding procedure. The model dependence of the unfolding is taken into account by adding to the systematic error the difference between the results obtained with PYTHIA, which are taken to be the central values, and PHOJET.

The $E_T^{\rm jet}$ distribution is compared to a NLO perturbative QCD calculation of the inclusive one-jet cross-section by Kleinwort and Kramer [5] who use the NLO GRV parametrisation of the photon structure function [6]. Their calculation was repeated for the kinematic conditions of this analysis. All scales are chosen to be equal to $E_T^{\rm jet}$. The strong coupling $\alpha_{\rm s}$ is calculated from the two-loop formula with $\Lambda^{(5)}_{\overline{\rm MS}} = 130$ MeV. The ratio of the NLO to the LO inclusive one-jet cross-section decreases from about 1.19 to 1.03 between $E_T^{\rm jet} = 3$ GeV and $E_T^{\rm jet} = 16$ GeV.

The direct, single- and double-resolved parts of the one-jet cross-section and their sum are shown separately. The agreement between data and the calculation is good. The resolved cross-sections dominate in the region $E_T^{\rm jet} \lesssim 5$ GeV, whereas, at high $E_T^{\rm jet}$ the direct cross-section is largest. The $E_T^{\rm jet}$ distribution falls less steeply than expected in γp and $\overline{\rm p}$p interactions, because the fraction of hard interactions rises from $\overline{\rm p}$p to γp to $\gamma\gamma$ interactions, due to the additional direct photon interactions. It should be noted that the NLO QCD calculation gives the jet cross-section for massless partons, whereas the jet cross-sections are measured for hadrons.

The inclusive two-jet cross-section is measured for events with at least 2 jets using the two jets with the highest $E_T^{\rm jet}$ in an event. The $E_T^{\rm jet}$ distribution is also compared to the NLO calculations [5], which have been extended to include the full NLO calculation for the double-resolved two-jet cross-section. The increase of the NLO compared to the LO inclusive two-jet cross-section is less than 10 % in the calculation.

The inclusive one- and two-jet cross-sections as a function of $|\eta^{\rm jet}|$ are shown in Fig. 4. Within the uncertainties of the measurement, the distributions are nearly independent of $|\eta^{\rm jet}|$ in agreement with the expectations of the Monte Carlo models.

The total cross-sections, which are dominated by the low $E_T^{\rm jet}$ events, depend on the photon structure function. In Fig. 4 the total jet cross-sections predicted by the two Monte Carlo models differ significantly even if the same photon structure function (here SaS-1D) is used. This model dependence reduces the sensitivity to the parametrisation of the photon structure function. Different parametrisations were used as input to the PHOJET simulation. The GRV-LO and SaS-1D parametrisations describe the data equally well, but the LAC1 parametrisation [7] overestimates the total jet cross-section by about a factor of two.

6 Conclusions

We have measured jet production in $\gamma\gamma$ interactions with the OPAL detector at $\sqrt{s}_{\rm ee}$ of 130 and 136 GeV, using a cone algorithm with $R = 1$, $E_T^{\rm jet} > 3$ GeV and $|\eta^{\rm jet}| < 1$.

Two-jet events originating from direct and resolved photon interactions were separated experimentally using $x_\gamma^{\pm}$. Jets in events with $\min(x_\gamma^+, x_\gamma^-) > 0.8$ are expected to be produced

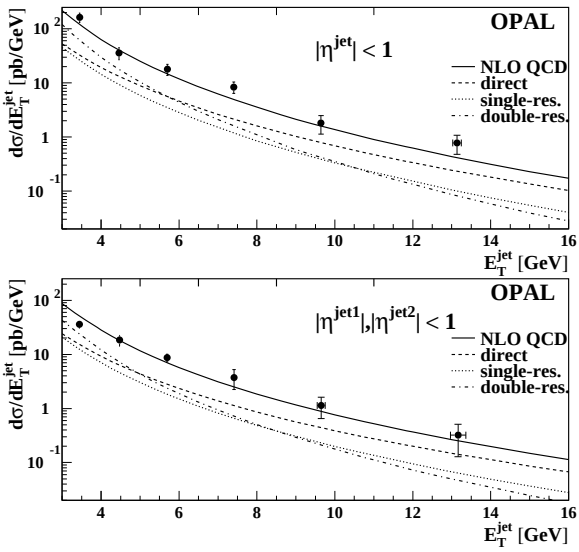

Figure 3: The inclusive one-jet (upper plot) and two-jet (lower plot) cross-sections as a function of $E_T^{\rm jet}$ compared to the NLO calculation by Kleinwort and Kramer [5]. The direct, single-resolved and double-resolved cross-sections and the sum are shown separately.

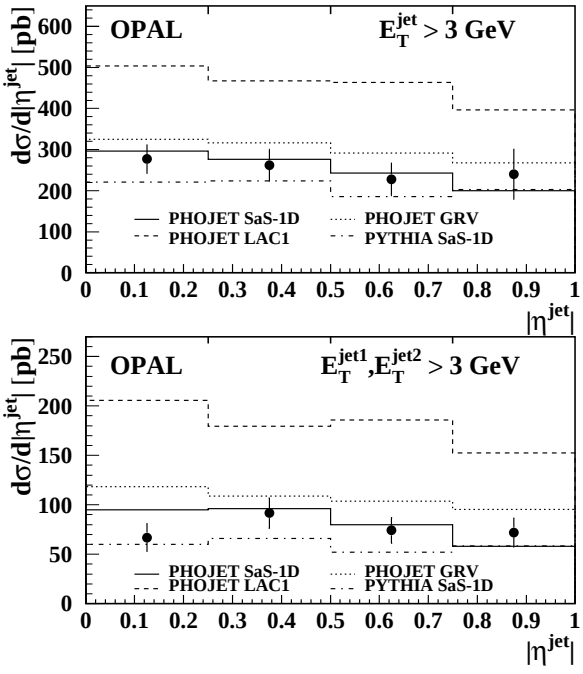

Figure 4: The inclusive one-jet (upper plot) and two-jet (lower plot) cross-sections as a function of $|\eta^{\rm jet}|$ compared to the LO QCD calculations of PYTHIA and PHOJET.

mainly from direct interactions. These jets are observed to have, on average, more average transverse energy and to be more collimated than jets in resolved events with $\min(x_\gamma^+, x_\gamma^-) < 0.8$. In resolved events a pedestal is observed in the transverse energy flows which may be related to the photon remnant. The Monte Carlo models PYTHIA and PHOJET describe the transverse energy flow distributions reasonably well.

The inclusive one-jet and two-jet production cross-sections were measured as a function of $E_T^{\rm jet}$ and $|\eta^{\rm jet}|$. The measurement extends the $E_T^{\rm jet}$ range of previous measurements [8] up to $E_T^{\rm jet} = 16$ GeV. The $E_T^{\rm jet}$ dependent one- and two-jet cross-sections are in good agreement with NLO QCD calculations [5].

Within the uncertainties of the measurements, the jet cross-sections are nearly independent of $|\eta^{\rm jet}|$ for $|\eta^{\rm jet}| < 1$. The total jet cross-section is dominated by the resolved cross-section. Given the model dependence of the jet cross-sections in PYTHIA and PHOJET, the GRV-LO and SaS-1D parametrisations describe the data equally well. The LAC1 parametrisation overestimates the total jet cross-section by about a factor of two.

References

1. T. Sjöstrand, *Comp. Phys. Commun.* 82 (1994) 74; G. A. Schuler and T. Sjöstrand, CERN-TH/96-119.
2. R. Engel and J. Ranft, ENSLAPP-A-540/95 and SI 95-08 (1995), to be publ. in *Phys. Rev.* D; R. Engel, *Z. Phys.* C66 (1995) 203.
3. ZEUS Collab., M. Derrick et al., *Phys. Lett.* B322 (1994) 287; H1 Collab., T. Ahmed et al., *Nucl. Phys.* B445 (1995) 195.
4. L. Lönnblad and M. Seymour (convenors), $\gamma\gamma$ *Event Generators*, in "Physics at LEP2", CERN 96-01, Vol. 2 (1996) 187.
5. T. Kleinwort and G. Kramer, DESY-96-035 (1996); *Phys. Lett.* B370 (1996) 141 and private communication.
6. M. Glück, E. Reya, A. Vogt, *Phys. Rev.* D46 (1992) 1973; *Phys. Rev.* D45 (1992) 3986.
7. H. Abramowicz, K. Charchula, A. Levy, *Phys. Lett.* B269 (1991) 458.
8. AMY Collab., B. J. Kim et al., *Phys. Lett.* B325 (1994) 248; TOPAZ Collab., H. Hayashii et al., *Phys. Lett.* B314 (1993) 149.